doi:10.1093/jmcb/mjz074
Published online July 22, 2019

Application Note

Systematical study of the mechanistic factors regulating genome dynamics *in vivo* by CRISPRsie

The spatiotemporal regulation of three-dimensional (3D) genome dynamics has been implicated in various genome functions including gene transcription, DNA recombination, DNA replication, and DNA repair (Bickmore, 2013). However, mechanistic studies to dissect the factors regulating genome dynamics and the causal roles of 3D genome structure in physiological processes have been significantly limited by experimental tools. Recently developed CRISPR/dCas9 genome labeling strategies allow the tracking of the particular genome regions in live cells (Chen et al., 2013). Various approaches have been developed to amplify the labeling signals and to reduce the non-specific backgrounds (Wu et al., 2019). In addition, dCas9 knock-in mouse strains were developed for tracking genome dynamics in live animals (Wang et al., 2016). However, most of the current dCas9 imaging studies are limited to reveal or confirm the correlations between dynamics of particular genome regions and its potential physiological functions, while more mechanistic studies are still required. To directly test the causal roles of 3D genome positioning in regulating genome functions, a CRISPR-GO system was developed recently to alter the nuclear localization of dCas9-targeted genome loci (Wang et al., 2018). On the other hand, the CRISPRii strategy was used to study the effect of silencing shelterin subunit on telomere dynamics *in vivo* (Duan et al., 2018). Previous studies demonstrated that in combination with truncated gRNAs, the catalytically active Cas9 could also behave like dCas9 and lead to targeted activation and repression (Dahlman et al., 2015; Kiani et al., 2015). We propose that such combination could also be used for genome labeling and extended for mechanistic study of factors regulating genome dynamics.

To test whether the truncation of gRNA (Dahlman et al., 2015; Kiani et al., 2015) could be used together with wild-type Cas9 (wtCas9) for *in vivo* genome labeling and imaging, we adapted the recently developed CRISPRainbow system (Ma et al., 2016) and replaced the dCas9 and full-length (22 nt) gRNA against human telomere repeats with wtCas9 and a 14-nt truncated gRNA lacking 5′ region, respectively (Supplementary Figure S1). A mCherry-TRF1 fusion was co-transfected to label the telomeres in HEK293T cells at the same time (Hong et al., 2018). The combination of wtCas9 and 14-nt telo-gRNA could efficiently and specifically label the telomeres in live cells (Figure 1A; Supplementary Figure S2A). Importantly, comparing with the original CRISP-Rainbow method, this 14-nt gRNA/wtCas9 combination showed similar numbers of telomere foci in each cell (Figure 1B), which also well co-localized with mCherry-TRF1 (Figure 1C) and showed similar signal-to-noise ratio (Supplementary Figure S2B).

To study the telomere dynamics in live animals, we delivered the telomere 14-nt gRNA and MS2 coat protein-green fluorescent protein (MCP-GFP) expression vector into Cas9 knock-in mouse (Platt et al., 2014) liver by hydrodynamic injection (Duan et al., 2018). After 48 h, the mice were anaesthetized, and liver lobes were exposured and imaged (Duan et al., 2018). Similar as the labeling in HEK293T cells, the 14-nt telo-gRNA could also efficiently label the telomeres in hepatocytes of live mice, which co-localized with co-injected BFP-TRF1 fusion protein very well (Supplementary Figure S3).

In addition, major satellite repeats (Supplementary Figure S4A and B) and other single genomic loci such as one in X chromosome could also be labeled efficiently by truncated gRNAs in Cas9 knock-in mice (Supplementary Figure S4C and D).

We hypothesized that combining the truncated gRNA targeting telomere repeats and full-length gRNAs targeting individual genes together with Cas9 knock-in mice could be used to dissect the roles of mechanistic factors in regulating telomere dynamics and their spatial localization *in vivo* (Figure 1D). The subunits of telosome/shelterin complex, such as TRF1, TRF2, and TIN2, play important roles in telomere length regulation and end protection (Takai et al., 2011). We generated piggyback vectors carrying the telomere 14-nt gRNA and full-length gRNAs targeting coding exons of various genes, as well as MCP-GFP expression cassettes. For each gene, four gRNAs were cloned into the same vector to achieve efficient knockout (Zuo et al., 2017). Delivering such constructs with hybase expression vector in mouse liver by hydrodynamic injection could lead to target-inactivation of coding genes, while in the same hepatocytes, the telomeres could be labeled by telo-gRNA and MCP-GFP. Consistent with previous results obtained from TRF1 conditionally inactivated mouse liver (Beier et al., 2015),

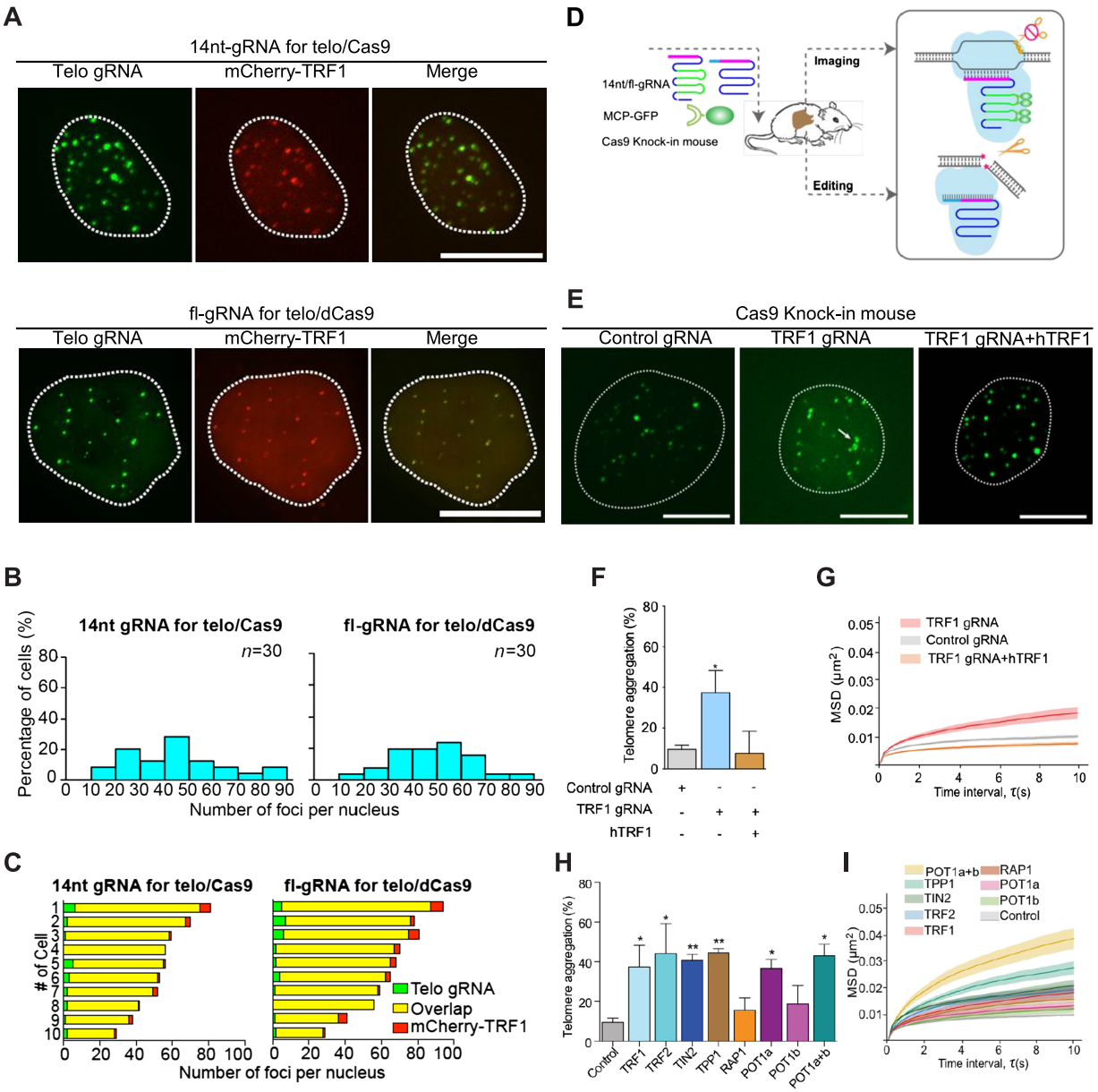

Figure 1 Systematical study of the mechanistic factors regulating genome dynamics *in vivo* by CRISPRsie. (**A**) Either 14-nt telo-gRNA against telomere repeats plus Cas9 (upper panel) or standard 22-nt full-length telomere gRNA plus dCas9 (lower panel) were transfected together with MCP-GFP into HEK293T cells to label the telomeres. The mCherry-TRF1 expression plasmid was co-transfected. Scale bar, 10 μm. (**B**) Histograms of telomere-labeling efficiency in HEK293T represented by puncta numbers in individual nuclei. $n = 30$ for each sample. (**C**) Quantification of telomere-labeling specificity in HEK293T based on co-localization with mCherry-TRF1 signals. (**D**) Schematic view of CRISPRsie. (**E**) Representative images of telomere aggregates (indicated by arrows) in mouse livers injected with control gRNA, TRF1 gRNAs, and TRF1 gRNAs + human TRF1 expression cassette. Scale bar, 10 μm. (**F**) Quantification of telomere aggregates in mouse livers injected with control gRNA ($n = 86$), TRF1 gRNAs ($n = 32$), and TRF1 gRNAs + human TRF1 expression cassette ($n = 24$). Two-sided *t*-test was used for statistical comparison. $^*P < 0.05$. (**G**) The average MSD curves of telomeres in Cas9 knock-in mice injected with control gRNA (319 foci collected in 22 cells from three mice), TRF1 gRNAs (111 foci collected in 17 cells from three mice), and TRF1 gRNAs+hTRF1 (251 foci collected in 19 cells from three mice). The data are displayed as mean ± SE. (**H**) Quantifications of telomere aggregates in mouse livers injected with control ($n = 86$), TRF1 ($n = 32$), TRF2 ($n = 57$), TIN2 ($n = 41$), TPP1 ($n = 32$), RAP1 ($n = 36$), POT1a ($n = 42$), POT1b ($n = 47$), and POT1a + POT1b gRNAs ($n = 30$). Two-sided *t*-test was used for statistical comparison. $^*P < 0.05$; $^{**}P < 0.01$. (**I**) The average MSD curves of telomeres in Cas9 knock-in mice injected with different gRNA constructs: TRF2 gRNA (81 foci collected in 14 cells from three mice), TIN2 (126 foci collected in 19 cells from three mice), TPP1 (124 foci collected in 16 cells from three mice), RAP1 (139 foci collected in 20 cells from three mice), POT1a (130 foci collected in 16 cells from three mice), POT1b (143 foci collected in 19 cells from three mice), and POT1a + POT1b (91 foci collected in 12 cells from three mice). The data are displayed as mean ± SE.

injection of TRF1-targeting gRNAs resulted in significantly increased telomere aggregates in hepatocytes *in vivo*, in comparison with control gRNA-injected samples (Figure 1E and F). In addition, inactivation of TRF1 by sgRNAs also led to significantly increased telomere dynamics revealed by mean-squared displacement (MSD) analysis (Figure 1G). Importantly, both telomere aggregation and increased dynamics could be rescued by overexpression of a human TRF1 cDNA (Figure 1F and G), which could not be targeted by mouse gRNAs. We then designed gRNAs to target-inactivate all individual telosome subunits. Inactivation of TRF1, TRF2, TIN2, TPP1, as well as POT1a, showed similarly increased telomere aggregations, while inactivation of RAP1 and POT1b did not significantly differ from control gRNAs (Figure 1H). Inactivation of individual telosome subunits also led to different alterations of telomere dynamics (Figure 1I; Supplementary Figure S5), which is not completely the same as the telomere aggregation phenotypes. Two functional distinct POT1 orthologs (POT1a and POT1b) have been identified in mouse. However, different from the results obtained in mouse embryonic fibroblasts (Hockemeyer et al., 2006), our data suggested that POT1a and POT1b synergistically regulated the telomere dynamics, while POT1a but not POT1b was mostly responsible for suppression of telomere fusion.

Here, we demonstrated that truncation of the 5′ region of gRNA could freeze the Cas9/gRNA/target complex in the cleavage-inactive intermediate state (Sternberg et al., 2015), which represents a new strategy for *in vivo* genome labeling and imaging. In addition, combining such truncated gRNA targeting telomere repeats and full-length gRNAs targeting individual candidate genes with Cas9 knock-in mice, the CRISPR simultaneously imaging and editing (CRISPRsie) strategy directly compared the roles of telosome/shelterin proteins in regulating telomere dynamics in live animals. Such method could be expanded to *in vivo* study the mechanistic factors regulating chromosome dynamics of other genomic regions in different tissues and cell types during physiological processes, such as X-chromosome inactivation and transcription regulation.

[Supplementary material is available at Journal of Molecular Cell Biology online. We thank Dr Minmin Luo (National Institute of Biological Sciences, Beijing) for reagents and members of Y.Z. laboratory for helpful discussion and support. This research was supported by the National Natural Science Foundation of China (81572795 and 81773304), the 'Hundred, Thousand and Ten Thousand Talent Project' by Beijing Municipal Government (2017A02), and the 'National Thousand Young Talents Program' of China to Y.Z. Q.H. is supported by the National Natural Science Foundation of China (31701135). We thank Beijing Municipal Government and the Ministry of Science and Technology of China for funds allocated to NIBS. D.H. and Y.Z. conceived the study. D.H., X.M., G.L., J.D., Y.H., Q.H., J.X., and X.S. performed experiments and analyzed data. Y.Z. analyzed data and wrote the manuscript with support from all authors.]

Deqiang Han[1], Yu Hong[1,2], Xueying Mai[1], Qingtao Hu[1], Guangqing Lu[1], Jinzhi Duan[1], Jingru Xu[1], Xiaofang Si[1,3], and Yu Zhang[1,2,3,4,*]

[1]National Institute of Biological Sciences, Beijing 102206, China
[2]Peking University–Tsinghua University–National Institute of Biological Sciences Joint Graduate Program, School of Life Sciences, Peking University, Beijing 100871, China
[3]Graduate School of Peking Union Medical College, Beijing 100730, China
[4]Tsinghua Institute of Multidisciplinary Biomedical Research, Tsinghua University, Beijing 100084, China
*Correspondence to: Yu Zhang, E-mail: zhangyu@nibs.ac.cn

Edited by Jinsong Li

References

Beier, F., Martinez, P., and Blasco, M.A. (2015). Chronic replicative stress induced by CCl4 in TRF1 knockout mice recapitulates the origin of large liver cell changes. J. Hepatol. *63*, 446–455.

Bickmore, W.A. (2013). The spatial organization of the human genome. Annu. Rev. Genomics Hum. Genet. *14*, 67–84.

Chen, B., Gilbert, L.A., Cimini, B.A., et al. (2013). Dynamic imaging of genomic loci in living human cells by an optimized CRISPR/Cas system. Cell *155*, 1479–1491.

Dahlman, J.E., Abudayyeh, O.O., Joung, J., et al. (2015). Orthogonal gene knockout and activation with a catalytically active Cas9 nuclease. Nat. Biotechnol. *33*, 1159–1161.

Duan, J., Lu, G., Hong, Y., et al. (2018). Live imaging and tracking of genome regions in CRISPR/dCas9 knock-in mice. Genome Biol. *19*,192.

Hockemeyer, D., Daniels, J.P., Takai, H., et al. (2006). Recent expansion of the telomeric complex in rodents: two distinct POT1 proteins protect mouse telomeres. Cell *126*, 63–77.

Hong, Y., Lu, G., Duan, J., et al. (2018). Comparison and optimization of CRISPR/dCas9/gRNA genome-labeling systems for live cell imaging. Genome Biol. *19*, 39.

Kiani, S., Chavez, A., Tuttle, M., et al. (2015). Cas9 gRNA engineering for genome editing, activation and repression. Nat. Methods *12*, 1051–1054.

Ma, H., Tu, L.C., Naseri, A., et al. (2016). Multiplexed labeling of genomic loci with dCas9 and engineered sgRNAs using CRISPRainbow. Nat. Biotechnol. *34*, 528–530.

Platt, R.J., Chen, S., Zhou, Y., et al. (2014). CRISPR-Cas9 knockin mice for genome editing and cancer modeling. Cell *159*, 440–455.

Sternberg, S.H., LaFrance, B., Kaplan, M., et al. (2015). Conformational control of DNA target cleavage by CRISPR-Cas9. Nature *527*, 110–113.

Takai, K.K., Kibe, T., Donigian, J.R., et al. (2011). Telomere protection by TPP1/POT1 requires tethering to TIN2. Mol. Cell *44*, 647–659.

Wang, H., La Russa, M., and Qi, L.S. (2016). CRISPR/Cas9 in genome editing and beyond. Annu. Rev. Biochem. *85*, 227–264.

Wang, H., Xu, X., Nguyen, C.M., et al. (2018). CRISPR-mediated programmable 3D genome positioning and nuclear organization. Cell *175*, 1405–1417.

Wu, X., Mao, S., Ying, Y., et al. (2019). Progress and challenges for live-cell imaging of genomic loci using CRISPR-based platforms. Genomics Proteomics Bioinformatics *17*, 119–128.

Zuo, E., Cai, Y.J., Li, K., et al. (2017). One-step generation of complete gene knockout mice and monkeys by CRISPR/Cas9-mediated gene editing with multiple sgRNAs. Cell Res. *27*, 933–945.